Design and control of a tri-axial miniature robot

N.C.A. Rabou*, I.S.M. Khalil

University of Twente, Faculty of Engineering Technology, Drienerlolaan 5, 7522 NB, Enschede, The Netherlands
**corresponding author n.c.a.rabou@student.utwente.nl*

ABSTRACT: The aim of this research is to find a state feedback control input to make the miniaturized tri-axial electromagnetic coil rotate controllably under the influence of static magnetic fields. A dynamical model was created in order to identify the influence of the environment on the tri-axial system. Some of these factors include, the external magnetic field and the fluid, as well as the influence of the design parameters, such as the design of the coils, the size of the capsule and the current input. Furthermore, the continuity and uniqueness of a solution of the system is analysed by means of the Lipschitz criteria. The system is proved to be globally Lipschitz continuous and therefore it is proven that there exists an unique solution for the control law in the states. The derived Lipschitz constant reveals insight on the influence of different parameters on the change of the behaviour of the system. Three different groups of parameters have been found to influence the systems behaviour namely design, electric and environment parameters. A control design is proposed which makes use of the nominal model of the dynamics and results in a complete controllable rotation of the tri-axial electromagnetic coils. The stability of the tri-axial system with the controller is proven by the Lyapunov's theorem. Therefore, the tri-axial micro-robot is able to rotate controllable with the proposed design.

Key words: tri-axial coil configuration, Non-linear systems, Lyapunov Stability, Lyapunov functions, Lipschitz Condition, rotational control, static magnetic fields

1 INTRODUCTION

In current medical practice, medical devices, such as micro-robots and untethered devices, enable clinicians to make use of minimally invasive surgery. Minimally invasive surgery refers to a surgical procedure which is performed through a small incision instead of a large cut. A small incision has many beneficial factors, such as reduction of recovery time and mitigation of several side-effects. One of the first minimally invasive procedures was implemented via tethered flexible endoscopes. In the last few decades, the progress in this field has increased exponentially [1].

One of these developments is the use of capsule endoscopy to acquire internal images of the gastrointestinal (GI) tract for medical diagnosis. The size of these capsules approaches a few centimeters, which is small enough to fit inside the GI system. This wireless capsule allows for a less invasive way of navigation in the body and can reach within the GI tract, which would be otherwise inaccessible for tethered flexible endoscopes. However, other natural pathways within the body, such as the circulatory system and the urinary system, are much smaller than the GI-tract. Therefore, the existing GI-tract devices cannot enter these tracts and must be down-scaled to micro-scale to allow them to access the smaller pathways. Naturally, down-scaling of these devices brings some challenges. One of these challenges is the limited space for propulsion mechanisms and on-board power sources. Therefore, there is a possibility that the device does not have the means for locomotion.

A solution to the above mentioned challenge can be solved by making use of an electromagnetic robot which translates magnetic forces and torques into motion. Research has been done into developing a miniature tetherless electromagnetic robot. This robot will consist of tri-axial electromagnetic coils (Figure 1), an embedded control system, power source, and an independent propulsion mechanism [2, 3]. The robot will be contained inside an electromagnetic configuration and static magnetic fields will be used to achieve directional control and propulsion inside fluids characterized by low Reynolds numbers. In almost all hospitals, a static magnetic field is already present as it can be generated by an MRI system. Therefore, the tri-axial miniature robot can easily be implemented into existing hospitals. By means of simulations, it has already been proven that it is possible to achieve directional control in an

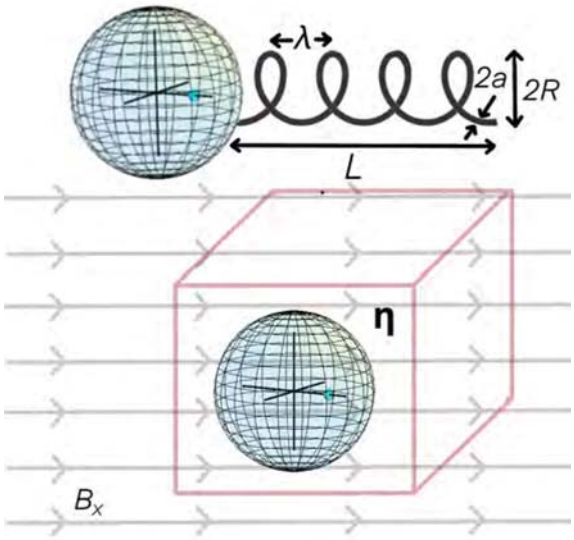

Fig. 1: The concept model includes tri-axial electromagnetic coils to achieve controllability of rotations around the axis when immersed inside a viscous fluid and a static magnetic field, $\mathbf{B} = [B_x, 0, 0]$. To translate the rotational movement into linear movement a helix tail is used, where L is the total length of the tail, λ the distance between two rotations, R the outer radius of the tail and a the radius of the material.

unidirectional nonuniform static magnet field using a controlled moment.

When a helical structure, as can been seen in figure 1 is attached to the capsule, a propulsive force can be generated when the capsule rotates about a certain axis. That force ensures the capsule to move in a certain direction. Therefore, the ultimate goal of this work is to demonstrate the ability of the capsule to rotate controllable under the influence of static magnetic fields. A nominal dynamic model will be used to design the control system and test its behavior numerically.

2 METHOD

A schematic overview of the tri-axial robot is displayed in figure 2. It consists of three axes. Each axis includes an electromagnetic coil and independent current input. The micro-robot will be located within an external unidirectional nonuniform field to be able to gain control over the micro-robot [3]. To ensure the rotational control over the micro robot, a control system has to be designed. Therefore, a dynamic model

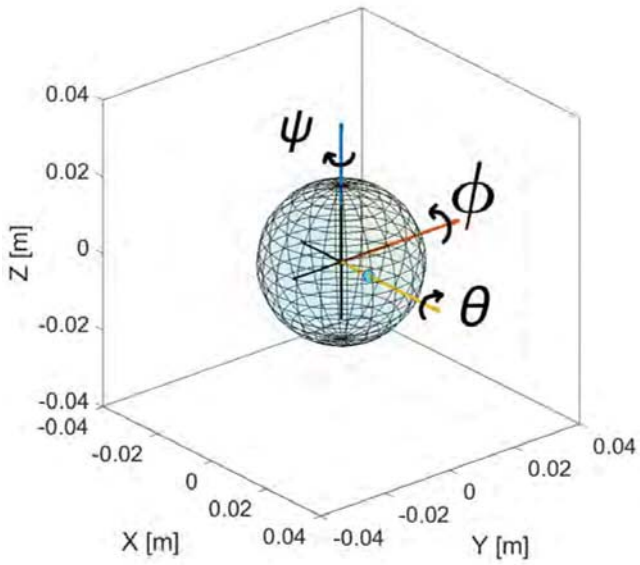

Fig. 2: Schematic overview of the tri-axial model with the corresponding Tait-Brian rotation angles.

is created, the behaviour of the system is analyzed by the Lipschitz criteria and the stability is tested by the Lyapunov theorem.

2.1 Dynamical model

As mentioned above, the micro-robot will be located within an external nonuniform field. Besides rotational movement of the capsule, the capsule will also experience linear movement due to the gradients present in the external magnetic field. The rotational movements take place due to the interaction between the external magnetic field and the dipole moments, $\mathbf{m} \in \mathbb{R}^{3\times1}$, generated by the electromagnetic coils. The dipole moments can be calculated by

$$\mathbf{m} = NS\mathbf{I}, \tag{1}$$

where N is the number of turns of the coil, S the total cross section of the coil and $\mathbf{I} \in \mathbb{R}^{3\times1}$ the current through each coil. When the micro-robot is located within the external magnetic field $\mathbf{B} \in \mathbb{R}^{3\times1}$, the magnetic dipole moment interacts with the magnetic field, generation a magnetic torque, $\boldsymbol{\tau_m} \in \mathbb{R}^{3\times1}$. This magnetic torque can be calculated by

$$\boldsymbol{\tau_m} = \mathbf{m} \times \mathbf{B}. \tag{2}$$

$$\begin{bmatrix}\dot{\phi}\\ \dot{\theta}\\ \dot{\psi}\end{bmatrix} = \frac{NS}{\pi d^3\eta}\begin{bmatrix}\frac{Bz(-\gamma Bz\sin\phi+\gamma Bx\sin\psi+1)-By(\gamma By\sin\phi-\gamma Bx\sin\theta+1)}{(\gamma Bz\sin\theta-By\sin\psi+1)^2+(-\gamma Bz\sin\phi+\gamma Bx\sin\psi+1)^2+(\gamma By\sin\phi-\gamma Bx\sin\theta+1)^2}\\ \frac{-Bz(\gamma Bz\sin\theta-By\sin\psi+1)+Bx(\gamma By\sin\phi-\gamma Bx\sin\theta+1)}{(\gamma Bz\sin\theta-By\sin\psi+1)^2+(-\gamma Bz\sin\phi+\gamma Bx\sin\psi+1)^2+(\gamma By\sin\phi-\gamma Bx\sin\theta+1)^2}\\ \frac{By(\gamma Bz\sin\theta-By\sin\psi+1)-Bx(-\gamma Bz\sin\phi+\gamma Bx\sin\psi+1)}{(\gamma Bz\sin\theta-By\sin\psi+1)^2+(-\gamma Bz\sin\phi+\gamma Bx\sin\psi+1)^2+(\gamma By\sin\phi-\gamma Bx\sin\theta+1)^2}\end{bmatrix}\mathbf{I}_{in} \tag{3}$$

Due to the non uniformity in the external field the micro-robot experiences a magnetic force that can be calculated using

$$\mathbf{f_m} = \nabla(\mathbf{B}\cdot\mathbf{m}), \tag{4}$$

where $\mathbf{f_m} \in \mathbb{R}^{3\times1}$ is the magnetic force acting on the micro-robot.

The micro-robot swims in low Reynolds numbers flows [2], therefore the drag force, $\mathbf{F}_d \in \mathbb{R}^{3\times1}$, and drag torque, $\tau_\mathbf{d} \in \mathbb{R}^{3\times1}$, can be calculated by

$$\mathbf{F}_d = 3\pi\eta d\dot{\mathbf{x}}, \tag{5}$$

$$\tau_d = \pi d^3\eta\mathbf{\Omega}, \tag{6}$$

respectively. Here η is the viscosity of the fluid, d the diameter of the micro-robot, $\dot{\mathbf{x}}$ the linear velocity and $\mathbf{\Omega}$ is the angular velocity of the micro-robot.

The angular velocity can also be written as

$$\mathbf{\Omega} = \begin{bmatrix}\dot{\phi}\\ \dot{\theta}\\ \dot{\psi}\end{bmatrix}, \tag{7}$$

where ϕ, θ and ψ are the Tait-Bryan angles which are used for the angles around the axes. A schematic overview of the Tait-Bryan angles is displayed in figure 2. ϕ repesents the rotation around the x-axis, θ around the y-axis and ψ around the z-axis. The three angles together are grouped as $\mathbf{\Theta}$.

For low Reynolds numbers, it can also be said that the only forces working on the micro-robot are the magnetic and the drag force and the only torques the magnetic and drag torques. Therefore, the equation of motion of the micro-robot can be written as:

$$\begin{aligned}\mathbf{f_m} + \mathbf{f_d} &= 0,\\ \boldsymbol{\tau_m} + \boldsymbol{\tau_d} &= 0.\end{aligned} \tag{8}$$

Using equation (8), the following linear dynamical system can be derived

$$\begin{bmatrix}\dot{x}_1\\ \dot{x}_2\\ \dot{x}_3\end{bmatrix} = \frac{NS}{3\pi d\eta}\begin{bmatrix}\frac{\partial}{\partial x}B_x & \frac{\partial}{\partial y}B_x & \frac{\partial}{\partial z}B_x\\ \frac{\partial}{\partial x}B_y & \frac{\partial}{\partial y}B_y & \frac{\partial}{\partial z}B_y\\ \frac{\partial}{\partial x}B_z & \frac{\partial}{\partial y}B_z & \frac{\partial}{\partial z}B_z\end{bmatrix}\mathbf{I}_{real}, \tag{9}$$

as well as the following rotational dynamical system

$$\begin{bmatrix}\dot{\phi}\\ \dot{\theta}\\ \dot{\psi}\end{bmatrix} = \frac{NS}{\pi d^3\eta}\begin{bmatrix}0 & B_z & -B_y\\ -B_z & 0 & B_x\\ B_y & -B_x & 0\end{bmatrix}\mathbf{I}_{real}. \tag{10}$$

The B_x represents the magnitude of the magnetic field in x-direction, B_y in y-direction and B_z in z-direction. Furthermore, $\mathbf{I}_{real}$ is the effective current that is used to make the tri-axial system move. This means that the back EMF, induced by the rotation of the coils in the external field, is taken into account. For $\mathbf{I}_{real}$ it holds that

$$\mathbf{I}_{real} = \mathbf{I}_{in} - \frac{2N|\mathbf{B}|S\sin\mathbf{\Theta\Omega}}{R}, \tag{11}$$

with $\mathbf{I}_{in}$ as the input current and R the resistance of the coils. Combining equation (10) with equation (11), gives the complete rotational dynamical model. This model is displayed in equation (3), with

$$\gamma = \frac{N^2|\mathbf{B}|S^2}{\pi d^3\eta R}. \tag{12}$$

In figure 3, the output of the electromagnetic tri-axial system without controller is displayed for three different input currents in an unidirectional uniform magnetic field. This means that the magnetic force is neglected for the moment. For the left plot an current is feed to the x-coil. As the external static magnetic field is orientated in the same direction as the x-coil, no motion will take place. For the middle and right plot an input is given to the y- and z-coil respectively. Both inputs do not result in the desired stable output.

Therefore, it can be concluded from figure 3 that the tri-axial system without controller is not

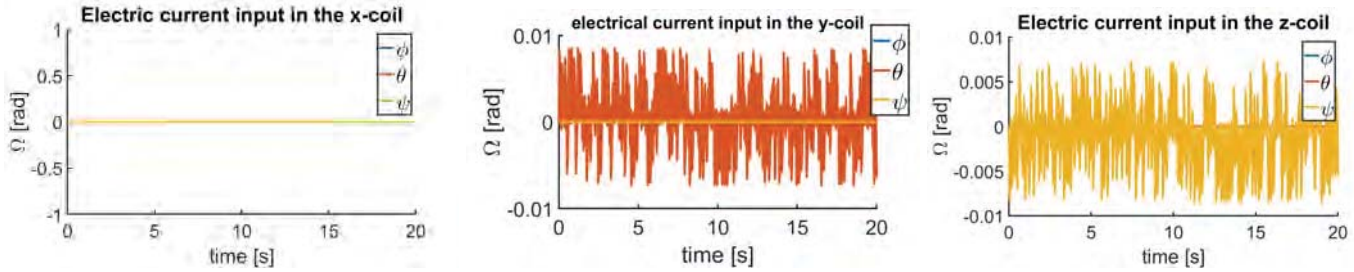

Fig. 3: The output of the electromagnetic tri-axial system without controller within a unidirectional uniform magnetic field $\mathbf{B} = [0.2, 0, 0]T$ for three different inputs, $\mathbf{I} = [35 \cdot 10^{-3}, 0, 0]$, $\mathbf{I} = [0, 35 \cdot 10^{-3}, 0]$, $\mathbf{I} = [0, 0, 35 \cdot 10^{-3}]$ respectively.

controllable. To obtain full directional control of the capsule, a controller should be designed. This controller should be designed in such a way that it outputs the current needed to acquire the desired rotation. The controller can be displayed using, C($\boldsymbol{\Theta}$(t)). In the following sections an analysis will be done to obtain a proper design for the controller.

2.2 Lipschitz condition

The Lipschitz condition is of great importance in many mathematical topics, such as geometric measure theory, partial differential equations and in nonlinear function analysis. It is used to test the existence and uniqueness of a solution [4].

The ultimate goal is to design a controller which will enable directional control of the tri-axial system. This means that every motion from the same starting point results in the exact same trajectory. Therefore, it has to be proven that the initial-value problem

$$\dot{\mathbf{x}} = f(t, \mathbf{x}), \quad \mathbf{x}(t_0) = \mathbf{x}_0, \tag{13}$$

has a unique solution via the Lipschitz condition [5]. The Lipschitz condition on an interval of [**x,y**] is given by [6]:

$$||f(\mathbf{x}, t) - f(\mathbf{y}, t)|| \leq L||\mathbf{x} - \mathbf{y}||. \tag{14}$$

A function, $f(\mathbf{x}, t)$ is called Lipschitz in the states if there exists a positive Lipschitz constant. The Lipschitz condition is used to to prove that there exists an unique solution for the control law. For this the Lipschitz constant is determined. It is assumed that

$$\begin{aligned} f(\mathbf{x}, t) &= \Omega(\mathbf{x}, t), \\ f(\mathbf{y}, t) &= \Omega(\mathbf{y}, t). \end{aligned} \tag{15}$$

A complex system arises from subtracting both functions. To be able to obtain the Lipschitz constant, some simplifications have been done.

The sine function is globablly Lipschitz as its derivative, cosine, is bounded by an upper limit with an absolute value of 1. Therefore, it holds that

$$\begin{aligned} sin(\mathbf{x}) &\leq 1, \\ sin(\mathbf{y}) &\leq 1. \end{aligned} \tag{16}$$

The sine can be replaced by this inequality since the Lipschitz condition is an inequality too. This simplification will not violate the original condition. Furthermore, it can be shown that the controller is sector bounded and we have

$$C(\mathbf{x}(t)) - C(\mathbf{y}(t)) \leq K|\mathbf{x} - \mathbf{y}|. \tag{17}$$

K is a constant representing the rate at which the control function changes. This change will also be bounded by the states.

Combining equations (16) and (17) into the Lipschitz inequality of equation (14), gives equation (18). The existence of the Lipschitz constant proves that for the tri-axial system there exists a unique solution which can smoothly vary within $\mathbb{R}^3$.

From the Lipschitz constant it can been seen that the solution of the tri-axial system with controller depends on the controller settings, the electrical parts, the magnetic field and the fluid in which it is located. To analyze the behaviour of the output better, the parameters are divided into different groups, namely design, electric and environment parameters. This division can be found in table 1.

$$L = \frac{KNS\sqrt{(B_x - B_y + B_x^2\gamma + B_y^2\gamma - B_y B_z\gamma)^2 + (B_x - B_z - B_x^2\gamma - B_z^2\gamma + B_x B_y\gamma + B_y B_z\gamma)^2 + (B_y - B_z + B_y^2\gamma + B_z^2\gamma - B_x B_y\gamma - B_x B_z\gamma)^2}}{d^3\eta\pi(2\gamma^2 B_x^2 - 2\gamma^2 B_x B_y - 2\gamma^2 B_x B_z + 2\gamma^2 B_y^2 - 2\gamma^2 B_y B_z + 2\gamma^2 B_z^2 + 3)} \quad (18)$$

Table 1: Division of the parameters of the Lipschitz constant

design	electric	environment
K	N	$B(B_x, B_y, B_z)$
d	S	η
	R	

The design parameters are the diameter, d, of the micro-robot and the control constant, K. A change in the diameter of the micro-robot, d has one of the largest influence on the solution of the the system. How smaller the diameter, the easier the micro-robot can rotate, the faster the solutions will change. This can be derived from the Lipschitz constant, as the diameter is under the division line. For the test setup it is aimed to design a prototype with a diameter of 25 mm.

In this stage, not much can be said about the control parameter yet as the control function is not yet known.

The electric parameters are the amount of turns, N, the total cross-section area of the coils, S, and the resistance, R, of the coils. When the amount of turns or the total area of the coils increases, the magnetic dipole moment of the coils will increase too. This can be derived from equation (1). A greater dipole moment will lead to a greater interaction between the coils and the external magnetic field, leading to a faster movement of the micro-robot. On the other hand, a higher resistance will ensure a slower movement of the micro-robot. This is because a higher resistance will decrease the efficiency of the coils and therefore result in a lower magnetic dipole moment.

These effects on the behaviour could also be derived from the Lipschitz constant, as N and S are above the division line and therefore a higher value resulting in a faster change of the system. While R is under the division line, decreasing the speed at which the system can change when it has a higher value. The optimal values of these parameters have been determined as $N = 280$, $S = a^2 - r^2(4 - \pi)$ with $a = 0.9$ cm and $b = 0.14$ cm and $R = 0.00216\ \Omega$ [7].

The environmental parameters are the magnetic field, B, and the viscosity, η. It holds that the stronger the external magnetic field, the faster the micro-robot will move. This also leads to a much faster changing system. This can not easily be concluded from the Lipschitz constant since there are magnetic field parameters above and below the division line.

A lower viscosity decreases the resistance of the fluid on the micro-robot, resulting in a lower drag force and torque. Therefore the micro-robot is able to move easier in a fluid with a lower viscosity compared to a fluid with a higher viscosity causing the tri-axial system to change more rapidly. This can also be concluded from the Lipschitz constant, as the viscosity term appears beneath the division line. For the test set up, silicone oil will be use, which has a dynamic viscosity of 8.2 - 5.5 Pa/s at $25\,^{\circ}\mathrm{C}$ -$35\,^{\circ}\mathrm{C}$ [8].

2.3 Lyapunov stability theorem

In the previous section it is proven that the system proposed in equation (3) is Lipschitz in the states and therefore that the tri-axial system has an unique solution on $\mathbb{R}^3$. The Lyapunov stabilitiy theorem is used to test the stability of Ordinary Differential Equations (ODEs), the existance of a so called Lyapunov function is enough to prove the stability of a system [9].

Lyapunov's stability theorem states that if there exists a continuously differentiable positive definitive function $V(\mathbf{x})$, for a dynamical system $\dot{\mathbf{x}} = f(\mathbf{x}, t)$, so that $V(\mathbf{x}, t) > 0$, $V(0) = 0$ and $\dot{V}(\mathbf{x}, t) \leq 0$, then $V(\mathbf{x})$ is a Lyapunov's function and thus the system is stable [10].

A Lyapunov's function describes a certain state, such as a enegery state, in which a system is. To obtain a stable system, one wants to have the system at a constant state or in a state that decreases towards zero. This is displayed in the criteria, $\dot{V}(\mathbf{x}, t) \leq 0$ and can be visualized by means of figure 4. In this figure the function, $V(\mathbf{x}) = C$ for $C \geq 0$, is displayed. $V(\mathbf{x}) = C$ describes a Lyapunov surface.

$$C = \frac{\pi d^3 \eta}{NS} \begin{bmatrix} \frac{Bz(-\gamma Bz\sin\phi+\gamma Bx\sin\psi+1)-By(\gamma By\sin\phi-\gamma Bx\sin\theta+1)}{(\gamma Bz\sin\theta-By\sin\psi+1)^2+(-\gamma Bz\sin\phi+\gamma Bx\sin\psi+1)^2+(\gamma By\sin\phi-\gamma Bx\sin\theta+1)^2} \\ \frac{-Bz(\gamma Bz\sin\theta-By\sin\psi+1)+Bx(\gamma By\sin\phi-\gamma Bx\sin\theta+1)}{(\gamma Bz\sin\theta-By\sin\psi+1)^2+(-\gamma Bz\sin\phi+\gamma Bx\sin\psi+1)^2+(\gamma By\sin\phi-\gamma Bx\sin\theta+1)^2} \\ \frac{By(\gamma Bz\sin\theta-By\sin\psi+1)-Bx(-\gamma Bz\sin\phi+\gamma Bx\sin\psi+1)}{(\gamma Bz\sin\theta-By\sin\psi+1)^2+(-\gamma Bz\sin\phi+\gamma Bx\sin\psi+1)^2+(\gamma By\sin\phi-\gamma Bx\sin\theta+1)^2} \end{bmatrix}^{-1} \begin{bmatrix} \dot{\phi}_{des} \\ \dot{\theta}_{des} \\ \dot{\psi}_{des} \end{bmatrix} \tag{19}$$

When the system crosses a certain Lyapunov surface, it will stay within this surface level because of the criteria $\dot{V}(\mathbf{x}, t) \leq 0$. Therefore, the system will keep decreasing towards the origin or any other equilibrium point [11].

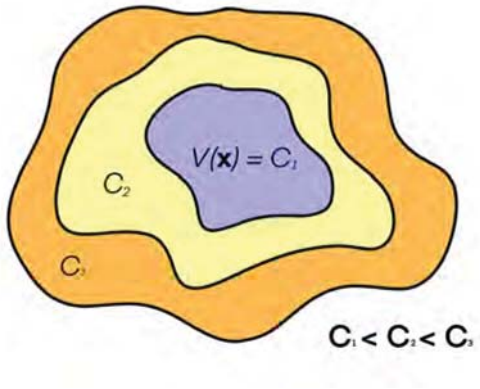

Fig. 4: Lyapunov surfaces for increasing values of k

A suitable suitable candidate for the Lyapunov's function for the tri-axial system would be

$$V(\mathbf{\Theta}) = \mathbf{\Theta}^T \mathbf{P} \mathbf{\Theta}$$
$$V(\mathbf{\Theta}) = \begin{bmatrix} \phi \\ \theta \\ \psi \end{bmatrix}^T \begin{bmatrix} p_{11} & p_{12} & p_{13} \\ p_{12} & p_{22} & p_{23} \\ p_{13} & p_{23} & p_{33} \end{bmatrix} \begin{bmatrix} \phi \\ \theta \\ \psi \end{bmatrix}. \tag{20}$$

$\mathbf{P} \in \mathbb{R}^{3\times3}$ is an arbitrarily chosen positive definite matrix for which it should hold that

$$\begin{aligned} &c_1||\mathbf{\Theta}|| \leq V(\mathbf{\Theta}) \leq c_2||\mathbf{\Theta}||^2, \\ &c_1 = (\lambda_{min}(\mathbf{P}^T\mathbf{P}))^{\frac{1}{2}}, \\ &c_2 = (\lambda_{max}(\mathbf{P}^T\mathbf{P}))^{\frac{1}{2}}. \end{aligned} \tag{21}$$

If the Lyapunov's function satisfies above mentioned criteria, then the time derivative is as follows

$$\begin{aligned} \dot{V}(\mathbf{\Theta}, t) = &\phi(2p_{11}\dot{\phi} + 2p_{12}\dot{\theta} + 2p_{13}\dot{\psi}) \\ &+ \theta(2p_{12}\dot{\phi} + 2p_{22}\dot{\theta} + 2p_{23}\dot{\psi}) \\ &+ \psi(2p_{13}\dot{\phi} + 2p_{23}\dot{\theta} + 2p_{33}\dot{\psi}) \end{aligned} \tag{22}$$

where $\dot{\mathbf{\Theta}}$ can be replaced by the derived system in equation (3).

3 RESULTS

3.1 Controller

The controller proposed in this article will be a controller which makes use of the nominal model of the dynamics. This results in a perfect controllable system. The controller function is displayed in equation (19), with $\dot{\phi}_{des}$, $\dot{\theta}_{des}$ and $\dot{\psi}_{des}$ as the desired angular velocities. Those desired angular velocities will be the input of the control system and are calculated by the derivative of the difference between the reference angle and the measured angle. The output of the controller is the current needed to make the micro-robot rotate controllable.

The block diagram of the tri-axial system with the implemented controller is shown in figure 8. The reference input of the system is the desired angle, Θ_{des}. When a mapped path is feed into the system in the shape of desired angles, full direction control of the capsule can be obtained.

In figures 5, 6 and 7, the output of the tri-axial system with controller located in a unidirectional uniform field in the x-direction is shown for different inputs. Figure 5 uses ϕ_{des} as reference input, which is a vector going from 0 to 8π in 5 seconds. This input results in four rotations around x-axis. It is shown that the output angles follow the reference angle perfectly, which proves that the controller ensures a controllable system.

For the input, figures 6 and 7 use θ_{des} and ψ_{des} respectively. These are also both vectors increasing from 0 to 8π in 5 seconds, causing four rotations around the y-axis in figure 6 and four rotations around the z-axis in figure 7. These figures also prove that the controller makes the system controllable.

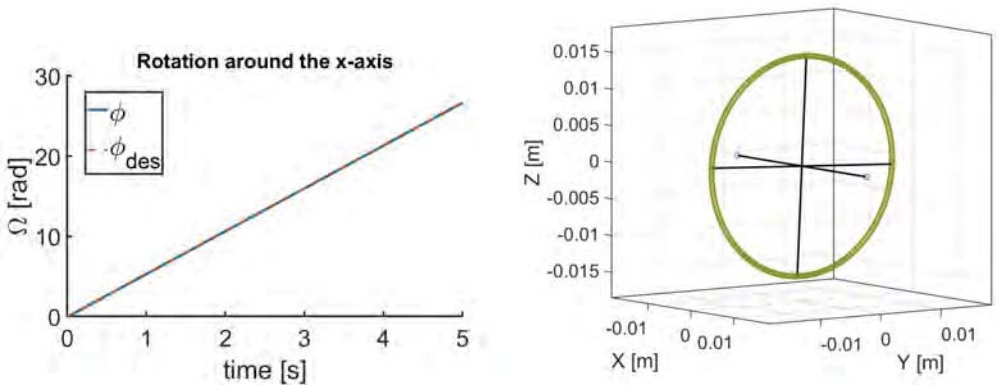

Fig. 5: System output of the electromagnetic tri-axial coil system with controller within a unidirectional uniform magnetic field $\mathbf{B} = [0.2, 0, 0]T$ rotating around the x-axis. The left plot shows the course of the rotation angle over time and the reference angle. The right plot shows how the electromagnetic coils move in time, with the colored dots displaying the displacement of the coils.

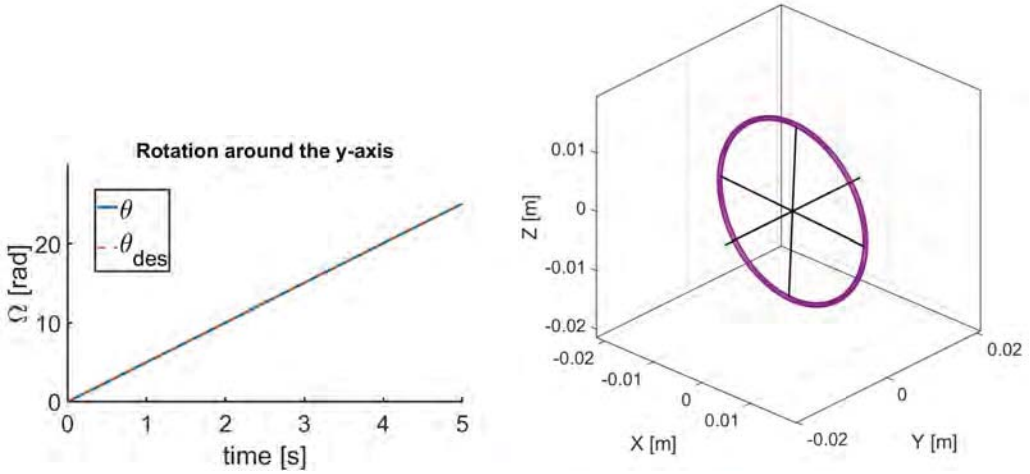

Fig. 6: System output of the electromagnetic tri-axial coil system with controller within a unidirectional uniform magnetic field $\mathbf{B} = [0.2, 0, 0]T$ rotating around the y-axis. The left plot shows the course of the rotation angle over time and the reference angle. The right plot shows how the electromagnetic coils move in time, with the colored dots displaying the displacement of the coils.

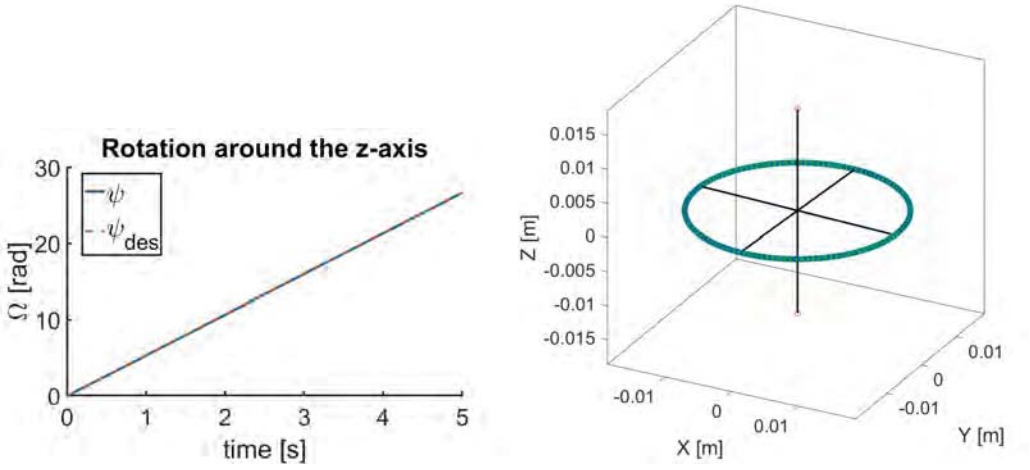

Fig. 7: System output of the electromagnetic tri-axial coil system with controller within a unidirectional uniform magnetic field $\mathbf{B} = [0.2, 0, 0]T$ rotating around the z-axis. The left plot shows the course of the rotation angle over time and the reference angle. The right plot shows how the electromagnetic coils move in time, with the colored dots displaying the displacement of the coils.

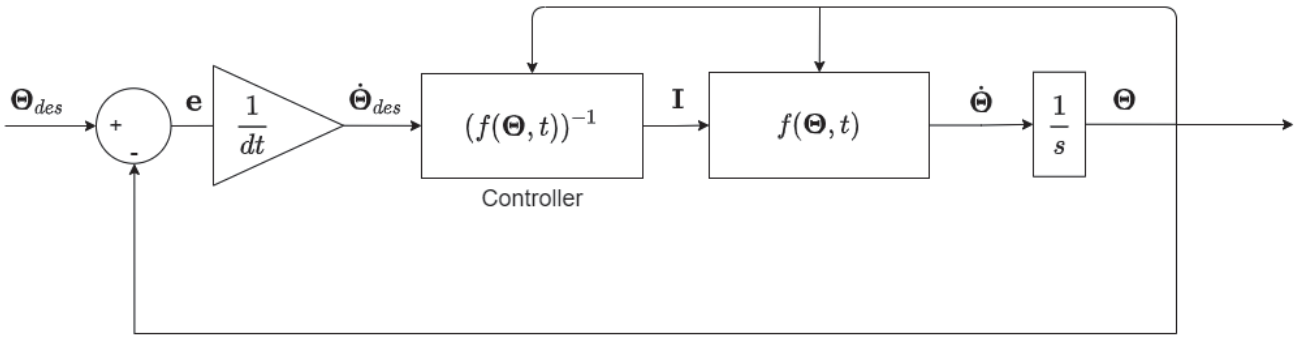

Fig. 8: Block diagram of tri-axial system with full state feedback control

3.2 Stability

For the Lyapunov function, the matrix

$$P = \begin{bmatrix} 1 & 4 & 3 \\ 4 & 1 & 2 \\ 3 & 2 & 1 \end{bmatrix} \tag{23}$$

has been chosen. This P matrix is positive definite as it is symmetric and all its eigenvalues are positive [12]. In figure 9, the Lyapunov's function of the tri-axial system with controller is plotted over time for a rotation around the y-axis. The bounds c_1 and c_2 are plotted as well, to see that the function meets the criteria of equation 20.

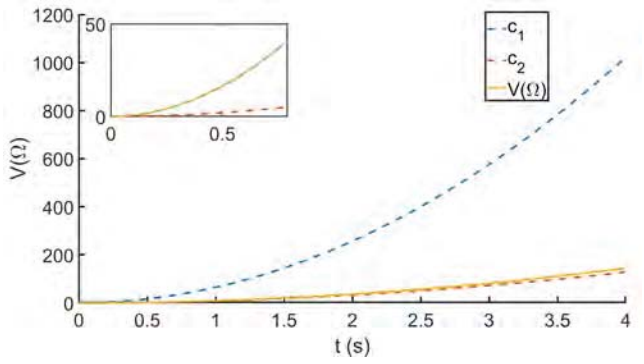

Fig. 9: Course of the Lyapunov's function for the rotation around the y-axis for the tri-axial system with the proposed controller over time, bounded by functions c_1 and c_2.

As mentioned in section 2.3, the stability of the tri-axial system can be achieved if there exists a Lyapunov's function. From figure 9 it can been seen that the Lyapunov's fuction of the tri-axial system meets the first two requirements, namely $V(\mathbf{\Omega}, t) > 0$ and $V(0) = 0$.

In figure 10, $\dot{V}(\Omega)$ is plotted against the time

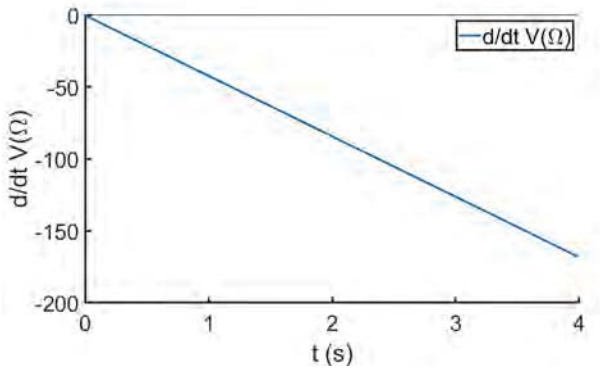

Fig. 10: Course of $\dot{V}(\Omega)$ with the proposed controller over time.

for a rotation around the y-axis. From this figure it becomes apparent that $\dot{V}(\mathbf{\Omega}, t) \leq 0$. Therefore, it can be concluded that the Lyapunov function as proposed in equation (20) is a suitable function for the tri-axial system. As there exists a Lyapunov's function for the system, the tri-axial system with controller is stable.

4 DISCUSSION

The results, shown in section 3, demonstrates that it is possible to make the capsule rotate controllable under the influence of a static magnetic field when the right controller is designed. The results are obtained by computer simulation and therefore perfect results can been seen in figures 5, 6 and 7. However, in practice, the proposed controller is very complex as it depends on many variables that should be measured by the system. Furthermore, in figure 5 it is shown that with controller the system is able to rotate around the x-axis. However, due to the external magnetic field which is directed in the x-direction, this could not be possible. As for the controller the inverse of the nominal model is used, the magnetic field parameters are

neglected, resulting in the ability of the system to rotate around the x-axis during simulations. For further research a new controller design should be thought of.

Furthermore, in the models as presented in this article, only uniform unidirectional magnetic fields are used. Therefore, the linear dynamic model is not taken into account and linear motion due to gradients in the magnetic field is ignored. During further research this should also be taken into account to see what the influence of this motion has on the behaviour and stability of the system.

5 CONCLUSION

In this thesis it has been proven that the low-Reynolds number dynamical system comprising a tri-axial electromagnetic coils in a unidirectional uniform magnetic field is Lipschitz on $\mathbb{R}^3$. Therefore, there exist a unique solution which can smoothly vary on $\mathbb{R}^3$. The behaviour of the solution can be evaluated and predicted with the use of the derived Lipschitz constant. In this article it is shown that the behaviour depends on design, electric and environment parameters. These parameters influence the ease with which the capsule can rotate and therefore the solution. The electric parameters mainly determine the magnitude of the interaction between the electromagnetic coils and the magnetic field. The design and environmental parameters influence the resistance the capsule experiences due to the interaction between the capsule and environmental.

The ability of the capsule to rotate controllable under the influence of static magnetic fields is achieved by the implementation of a controller that makes use of the nominal model of the dynamics. The use of this controller realizes a stable system, which was proven by the Lyapunov's criteria.

6 FUTURE WORK

For future work, a simpler control design should be used to obtain the desired rotational movement of the capsule. Furthermore, the simulation should be run again with a non-uniform unidirectional static magnetic field instead of a uniform field to see how this influences the results. A prototype should be build to validate the finding of this research.

REFERENCES

1. O.H. Hamed, N.J. Gusani, E.T. Kimchi, and S.M. Kavic, Minimally invasive surgery in gastrointestinal cancer: Ben-efits, challenges, and solutions for underutilization, *Journal of the Society of Laparoendoscopic Surgeons*, (2014), 18(4).
2. A. Harbers and I.S.M Khalil, Control of a thertherless miniature robot using static mangetic fields, *ME Bachelor Assignments proceedings 1&2 July*, (2020).
3. E. Hopman and I.S.M Khalil, Directional control of a minia-ture tri-axial electromagnetic coil in a static magnetic field, *ME Bachelor Assignments proceedings 1&2 July*, (2020).
4. J. Heinonen, *Lecture on Lipschitz analysis*, (100).
5. Hassan K Khalil and Jessy W Grizzle, *Nonlinear systems*, volume 3, Prentice hall Upper Saddle River,
6. NJ, (2002). A.S. Poznyak, *Advanced Mathematical Tools for Automatic Control Engineers: Deterministic Techniques*, Elsevier,(2008).
7. Awg american wire gauge diameter and resistance, https://www.daycounter.com/Calculators/AWG.phtml, (2019), Accessed: 17 June, 2021.
8. S. Zhai, L. Song, and X. Lv, Measurements and analysis of silicone oil, characteristics and viscosity-temperature index, *IOP Conference Series:Earth and Environmental Science*, nov 2019, 330:32–49.
9. L.T. Grujic, Solutions to lyapunov stability problems: non-linear systems with continuous motions, *Internat. J. Math & Math. Sci.*, (1994), 17(3):587–596.
10. H.K. Khalil, Lyapunov stability, *Control Systems, Robotics and AutomatioN-Volume XII: Nonlinear, Distributed and Time Delay Systems-I*, (2019), 115.
11. E. Hossain, R. Perez, S. Padmanban, L. Mihet-Popa, Blaabjerg, and B.K. Ramachandaramurthy, Sliding mode controller and lyapunov redesign controller to improve mi-crogrid stability: A comparative analysis with cpl power variation, *Energies*, nov 2017, 10(1959).
12. D. Zwick, Lecture 33: Positive definite matrices, *Math 2270*, (2012).
13. I. S. M. Khalil, A. Klingner, and S. Misra, Mathematical modeling of swimming soft microrobots, *Academic Press*, (2021).